

INFLUENCE OF DATA ACQUISITION ALGORITHMS ON X-RAY PHASE CONTRAST IMAGING COMPUTED TOMOGRAPHY

Collin J. C. Epstein*, Ryan N. Goodner, Kyle R. Thompson, Amber L. Dagel
Sandia National Laboratories
Albuquerque, New Mexico 87123

ABSTRACT

X-ray phase contrast imaging (XPCI) is a non-destructive evaluation technique that enables high-contrast detection of low-density materials that are transparent to traditional radiography. Extending a grating-based XPCI system to three-dimensional imaging with computed tomography (CT) imposes two stage motion requirements: the analyzer grating must translate transverse to the system optical axis to capture images sets for XPCI reconstruction, and the sample stage must rotate to capture angular data for CT reconstruction. The motion of both stages are determined by the acquisition algorithm used in the system. Therefore, the design of image acquisition algorithms for XPCI CT is instrumental to collecting high fidelity data for reconstruction. We investigate how data acquisition influences XPCI CT by comparing two simple data acquisition algorithms.

1 INTRODUCTION

X-ray phase contrast imaging (XPCI) is a radiography technique that leverages the wave properties of X-rays to obtain phase contrast data in addition to traditional absorption contrast data. In the hard X-ray regime, the phase cross-section can exceed the attenuation cross-section by up to three orders of magnitude for elements with low atomic numbers [1]. Volumetric reconstructions of XPCI data can be reconstructed using computed tomography (CT) techniques [2], which include capturing numerous angular samples of a rotating object.

We implement a laboratory table-top grating-based XPCI system using a Talbot-Lau interferometer [3, 4] (Fig. 1). The interferometer creates a fringe pattern on the detector. Phase

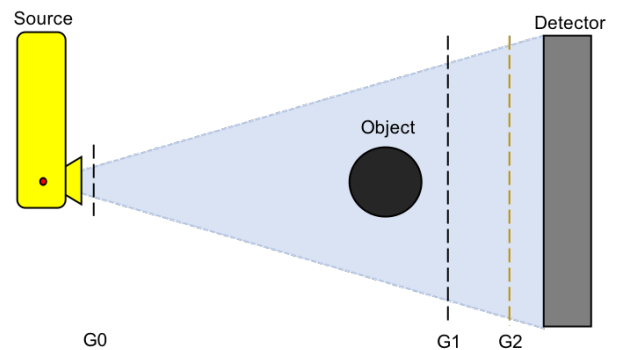


FIGURE 1. GRATING-BASED XPCI APPARATUS DIAGRAM. ANALYZER GRATING G_2 TRANSLATES TO MOVE FRINGES.

reconstruction requires the acquisition of a sequence of images captured as the analyzer grating G_2 translates transverse to the optical axis of the system. The movement of G_2 causes lateral movement of the fringe pattern. We capture the requisite images for XPCI reconstruction by translating the grating over a full grating period at regular intervals and capturing a radiograph at each grating position.

XPCI reconstruction results in three image products: absorption, dark field, and differential phase (Fig. 2). The absorption image is equivalent to traditional attenuation-contrast radiography, the dark field image is due to small-angle scatter, and the differential phase image reveals material interfaces.

The combination of interferometer motion required for grating-based XPCI and sample rotation mandated by CT dictates at least two distinct image acquisition algorithms: capture

*Email: cepstei@sandia.gov

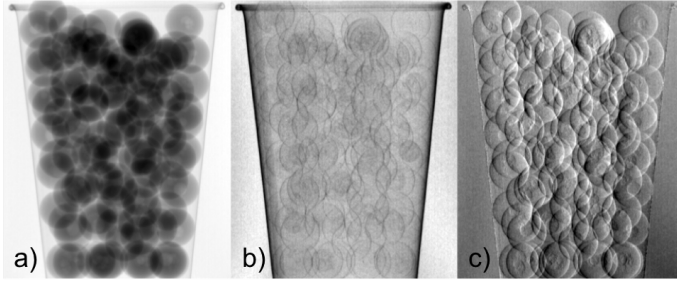


FIGURE 2. EXAMPLE: POLYPROPYLENE SPHERES IN CUP.
a) ABSORPTION b) DARK FIELD c) DIFFERENTIAL PHASE
SINGLE DATASET YIELDS THREE IMAGING MODES.

an entire phase image set before rotating the object to a new angle, or capture an entire sample rotation at a given grating position before moving the grating. We examine the influence of data acquisition algorithm choice on XPCI CT reconstruction by comparing the performance of two image acquisition algorithms.

In this investigation, we examine a paper cup containing polypropylene spheres as a sample object (Fig. 2).

2 DATA ACQUISITION ALGORITHMS

XPCI CT requires the acquisition of images that satisfy both XPCI and CT reconstruction requirements. The image data must include radiograph sets acquired for each rotary position, or projection, of the sample, and each projection image set must contain an image set adequate for XPCI reconstruction of that projection. Therefore, data acquisition algorithms must coordinate two mechanical stages: the analyzer grating G_2 horizontal translation stage, and the sample rotational mount.

2.1 Nested Loop Organization

The motion requirements for XPCI CT indicate that each stage may be considered as a motion loop, a set of movements that could be executed repeatedly. The organization of potential data acquisition algorithms might then follow a nested loop form in which one motion loop executes within the other. Two acquisition algorithms are then readily apparent: one in which sample rotation is the outer loop and grating translation is the inner loop (*PhaseCT1*, Alg. 1), and vice versa (*PhaseCT2*, Alg. 2). Numerous other data acquisition algorithms for XPCI CT have been explored, including interlaced grating translation [5, 6], helical XPCI CT [7], and no grating movement at all [8]. We consider the two simple nested loop algorithms *PhaseCT1* and *PhaseCT2*.

2.2 Algorithm Comparison

The two data acquisition algorithms should capture the same images in a different order. Nevertheless, there are distinct advantages and disadvantages to each algorithm. If a *PhaseCT1*

ALGORITHM 1 *PHASECT1* ACQUISITION ALGORITHM

Input: User-defined acquisition parameters

Output: XPCI CT image set

- 1: **for** $i := 0$ to $CT\ projections$ **do**
 - 2: move rotary stage to i th projection angle
 - 3: **for** $j := 0$ to $G_2\ positions$ **do**
 - 4: move analyzer grating stage to j th position
 - 5: acquire radiograph
 - 6: **end for**
 - 7: **end for**
-

ALGORITHM 2 *PHASECT2* ACQUISITION ALGORITHM

Input: User-defined acquisition parameters

Output: XPCI CT image set

- 1: **for** $i := 0$ to $G_2\ positions$ **do**
 - 2: move analyzer grating stage to i th position
 - 3: **for** $j := 0$ to $CT\ projections$ **do**
 - 4: move rotary stage to j th projection angle
 - 5: acquire radiograph
 - 6: **end for**
 - 7: **end for**
-

scan fails and doesn't capture an entire image set, the incomplete data would include a subset of projections with complete data for XPCI reconstruction. In the event that sufficient complete projections were captured, a limited-angle CT scan of that data set could still be reconstructed. On the other hand, a failed *PhaseCT2* scan results in an incomplete data set that cannot be reconstructed into XPCI image products, since no individual projection would have sufficient data for XPCI reconstruction. A traditional absorption CT scan could potentially be reconstructed from a single sample rotation, but only the absorption image would be available and the visible fringes would introduce significant reconstruction artifacts. However, *PhaseCT2* offers the potential for shorter scan times compared to *PhaseCT1*. If the scan runs at a high frame rate, *PhaseCT2* could rotate the sample continuously, with the grating translating to the next position at the conclusion of each sample revolution.

In practice, the data captured by the two acquisition algorithms differ slightly due to system error. For long exposures, the image calibrations expire towards the end of the scan, resulting in slightly noisier reconstructed projections towards the end of a long *PhaseCT1* scan. Additionally, minute changes in grating positioning between projections results in noticeable variations in the reconstructed differential phase images (Fig. 3). The distinct horizontal bands in the *PhaseCT1* sinogram indicate variability in brightness and/or image gradient between projections. Notice that the *PhaseCT2* sinogram lacks similar banding. Since the grating remains in the same location for all projections in a given rotation in *PhaseCT2*, the variability in sample signal due to grating movement is reduced. The uniform projection inten-

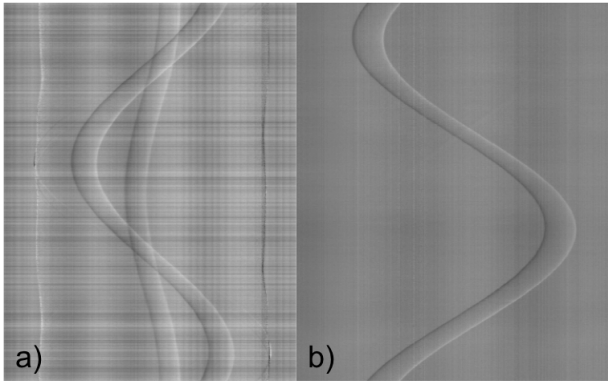


FIGURE 3. POLYPROPYLENE SPHERES SINOGRAMS
a) PHASECT1 ACQUISITION b) PHASECT2 ACQUISITION
HORIZONTAL STRIPES INTRODUCE IMAGE ARTIFACTS.

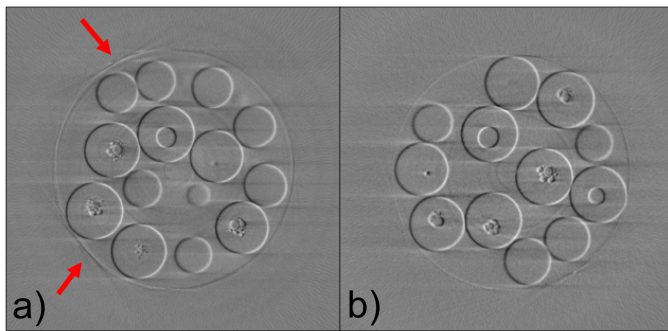


FIGURE 4. POLYPROPYLENE SPHERE RECONSTRUCTIONS
a) PHASECT1 ACQUISITION b) PHASECT2 ACQUISITION
RED ARROWS INDICATE STREAKING ARTIFACTS.

sity results in superior differential phase CT reconstructions using *PhaseCT2* (Fig. 4). The diagonal streaking artifacts seen in the *PhaseCT1* reconstruction are reduced in the *PhaseCT2* reconstruction. Additionally, the ring artifacts present in the *PhaseCT1* reconstruction appear to be suppressed in the *PhaseCT2* scan. The horizontal streak artifacts present in both images are a consequence of reconstructing only 180° of projection data.

3 CONCLUSION

XPCI CT for a system based on a Talbot-Lau interferometer requires multiple moving stages to acquire the requisite data for successful reconstruction. Coordination of those stages demands deliberate attention to the design of data acquisition algorithms and their effects on the resulting image sets.

While the choice of whether to place grating translation or sample rotation in the inner or outer acquisition loops primarily determines the order in which scan images are captured, it can also influence the XPCI CT reconstruction. *PhaseCT1* results in

data sets that can be salvaged in the event of a failed scan, while *PhaseCT2* delivers cleaner reconstructions. We prefer *PhaseCT2* when pursuing high-quality volume data.

ACKNOWLEDGMENTS

This paper describes objective technical results and analysis. Any subjective views or opinions that might be expressed in the paper do not necessarily represent the views of the U.S. Department of Energy or the United States Government.

This work was supported by the Laboratory Directed Research and Development program at Sandia National Laboratories. Sandia National Laboratories is a multimission laboratory managed and operated by National Technology & Engineering Solutions of Sandia, LLC, a wholly owned subsidiary of Honeywell International Inc., for the U.S. Department of Energy's National Nuclear Security Administration under contract DE-NA0003525.

SAND2019-4036 C

REFERENCES

- [1] Momose, A., 2005. "Recent advances in x-ray phase imaging". *Japanese Journal of Applied Physics*, **44**(9A), pp. 6355–6367.
- [2] Pfeiffer, F., Bunk, O., Kottler, C., and David, C., 2007. "Tomographic reconstruction of three-dimensional objects from hard X-ray differential phase contrast projection images". *Nuclear Instruments and Methods in Physics Research, Section A: Accelerators, Spectrometers, Detectors and Associated Equipment*, **580**(2), pp. 925–928.
- [3] Pfeiffer, F., Weitkamp, T., Bunk, O., and David, C., 2006. "Phase retrieval and differential phase-contrast imaging with low-brilliance x-ray sources". *Nature physics*, **2**(4), p. 258.
- [4] Pfeiffer, F., Kottler, C., Bunk, O., and David, C., 2007. "Hard X-ray phase tomography with low-brilliance sources". *Physical Review Letters*, **98**(10).
- [5] Zanette, I., Bech, M., Pfeiffer, F., and Weitkamp, T., 2011. "Interlaced phase stepping in phase-contrast x-ray tomography". *Applied Physics Letters*, **98**(9), pp. 2009–2012.
- [6] Zanette, I., Bech, M., Rack, A., Le Duc, G., Tafforeau, P., David, C., Mohr, J., Pfeiffer, F., and Weitkamp, T., 2012. "Trimodal low-dose X-ray tomography". *Proceedings of the National Academy of Sciences*, **109**(26), pp. 10199–10204.
- [7] Fu, J., Willner, M., Chen, L., Tan, R., Achterhold, K., Bech, M., Herzen, J., Kunka, D., Mohr, J., and Pfeiffer, F., 2014. "Helical differential X-ray phase-contrast computed tomography". *Physica Medica*, **30**(3), pp. 374–379.
- [8] Bevins, N., Zambelli, J., Li, K., Qi, Z., and Chen, G. H., 2012. "Multicontrast x-ray computed tomography imaging using Talbot-Lau interferometry without phase stepping". *Medical Physics*, **39**(1), pp. 424–428.